Article

Methodology for Synthesizing Crystalline Metallosilicates with Expanded Pore Windows Through Molecular Alkoxysilylation of Zeolitic Lamellar Precursors

Peng Wu, Juanfang Ruan, Lingling Wang, LeiLei Wu, Yong Wang, Yueming Liu, Weibin Fan, Mingyuan He, Osamu Terasaki, and Takashi Tatsumi

J. Am. Chem. Soc., **2008**, 130 (26), 8178-8187 • DOI: 10.1021/ja0758739 • Publication Date (Web): 04 June 2008

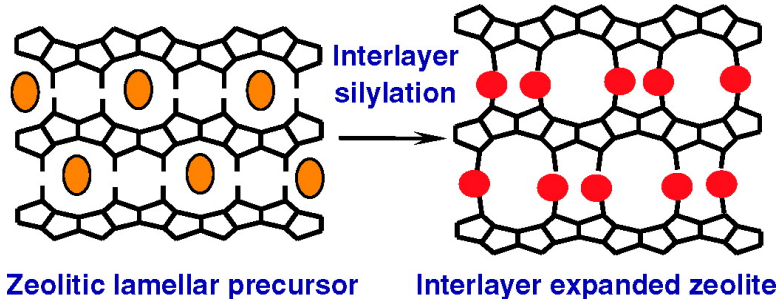

More About This Article

Additional resources and features associated with this article are available within the HTML version:

- Supporting Information
- Access to high resolution figures
- Links to articles and content related to this article
- Copyright permission to reproduce figures and/or text from this article

View the Full Text HTML

J|A|C|S
ARTICLES

Published on Web 06/04/2008

Methodology for Synthesizing Crystalline Metallosilicates with Expanded Pore Windows Through Molecular Alkoxysilylation of Zeolitic Lamellar Precursors

Peng Wu,*,† Juanfang Ruan,‡ Lingling Wang,† LeiLei Wu,† Yong Wang, Yueming Liu,† Weibin Fan,§ Mingyuan He,† Osamu Terasaki,‡ and Takashi Tatsumi§

Shanghai Key Laboratory of Green Chemistry and Chemical Processes, Department of Chemistry, East China Normal University, North Zhongshan Rd 3663, Shanghai 200062, China, Structural Chemistry, Arrhenius Laboratory, Stockholm University, 10691 Stockholm, Sweden, and Chemical Resources Laboratory, Tokyo Institute of Technology, 4259 Nagatsuda-chu, Midori-ku, Yokohama 226-8503, Japan

Received August 9, 2007; E-mail: pwu@chem.ecnu.edu.cn

Abstract: Postalkoxysilylation with diethoxydimethylsilane has been carried out on the zeolitic lamellar precursors of various topologies such as MWW, FER, CDO and MCM-47 aiming to construct new crystalline structures with expanded pore apertures between the layers. The silylation process and the crystalline and pore structures of the resulting materials have been investigated with the techniques of XRD, IR, ^{13}C and ^{29}Si MAS NMR, ICP, SEM, HRTEM, elemental analyses, and N_2 adsorption. In contrast to forming known three-dimensional zeolite structures after direct calcination of the lamellar precursors, the silylation led to new crystalline structures with opener pores, as evidenced by the shift of layer-related diffractions to the lower-angle region in XRD patterns and the enlarged interlayer pores found by HRTEM images. After optimizing the treatment conditions, particularly the amount of silane agent, a maximum and homogeneous silylation was realized, which guaranteed the phase purity in interlayer expanded zeolites. The expanded structures were well preserved after calcination at 823 K or reflux in water for 1 to 2 weeks, indicating a high thermal stability and also a hydrothermal stability. The interlayer expanded zeolites prepared from the metallosilicate precursors of MWW topology exhibited higher catalytic activities in the redox and solid acid-catalyzed reactions of bulky molecules than that of their counterparts with conventional MWW topology.

1. Introduction

Zeolites are a class of important microporous crystalline materials which serve as promising adsorbents, ion-exchangers, catalyst supports, and especially active and selective catalysts.[1] It has been and will continue to be a great challenge to develop new zeolite structures with unique porosity, if possible with micropores larger than a 10-membered ring (MR), for the purpose of processing bulky reactant molecules as solid acid and redox catalysts as well as providing selective adsorbents for separation. Through designing organic structure-directing agents (SDAs) and/or with the combination of crystallization-supporting metal ions, for example Ge is capable of constructing readily double 4 MR units hardly formed by Si alone, the direct hydrothermal synthesis has been established as the most effective, widely adopted method.[1–3] It may be possible to modify the known zeolites or to convert them to new three-dimensional (3D) crystalline zeolite structures by postmodification. However, this kind of conversion is limited mostly because of their relatively "rigid and hard" frameworks, with the exception of zeolites that have lamellar sheets as their structural unit. The zeolites, originating from lamellar precursors, e.g., MCM-22 (MWW),[4] ferrierite (FER),[5] Nu-6(2) (NSI),[6] CDS-1 (CDO),[7] MCM-47,[8] ERS-12,[9] MCM-65,[10] RUB-41 (RRO),[11] and layered aluminofluorophosphate (AFO)[12] are already known, and they are possibly subject to structural

† Department of Chemistry, East China Normal University, China.
‡ Structural Chemistry, Stockholm University, Sweden.
§ Chemical Resources Laboratory, Tokyo Institute of Technology, Japan.

(1) Davis, M. E. *Nature* **2002**, *417*, 813–821.
(2) (a) Corma, A.; Diaz-Cabañas, M. J.; Martínez-Triguero, J.; Rey, F.; Rius, J. *Nature* **2002**, *418*, 514–517. (b) Corma, A.; Rey, F.; Valencia, S.; Jordá, J.; Rius, J. *Nat. Mater.* **2003**, *2*, 493–497.
(3) Burton, A. *Nat. Mater.* **2003**, *2*, 438–440.
(4) Leonowicz, M. E.; Lawton, J. A.; Lawton, S. L.; Rubin, M. K. *Science* **1994**, *264*, 1910–1913.
(5) Schreyeck, L.; Caullet, P. H.; Mougenel, J. C.; Guth, J. L.; Marler, B. *Microporous Mater.* **1996**, *6*, 259–271.
(6) Zanarrdi, S.; Alberti, A.; Cruciani, G.; Corma, A.; Fornés, V.; Brunelli, M. *Angew. Chem., Int. Ed.* **2004**, *43*, 4933–4937.
(7) Ikeda, T.; Akiyama, Y.; Oumi, Y.; Kawai, A.; Mizukami, F. *Angew. Chem., Int. Ed.* **2004**, *43*, 4892–4896.
(8) Burton, A.; Accardi, R. J.; Lobo, R. F. *Chem. Mater.* **2002**, *12*, 2936–2942.
(9) Millini, R.; Carluccio, L. C.; Carati, A.; Bellussi, G.; Perego, C.; Cruciani, G.; Zanardi, S. *Microporous Mesoporous Mater.* **2004**, *74*, 59–71.
(10) Dorset, D. L.; Kennedy, G. J. *J. Phys. Chem. B* **2004**, *108*, 15216–15222.
(11) Wang, Y. X.; Gies, H.; Marler, B.; Müller, U. *Chem. Mater.* **2005**, *17*, 43–49.
(12) Wheatley, P. S.; Morris, R. E. *J. Mater. Chem.* **2006**, *16*, 1035–1037.

10.1021/ja0758739 CCC: $40.75

modifications. With the increase in number, these kinds of zeolites are gradually forming an important family of microporous materials. As a representative among them, the MWW-type aluminosilicate, well-known as MCM-22, has already found important industrial applications to the selective production of bulk petrochemicals such as cumene and ethylbenzene.[13] However, the recently developed MWW-type titanosilicate, Ti-MWW, has been demonstrated to be an effective catalyst for the epoxidation of various alkenes and ammoximation of ketones using hydrogen peroxide as a clean oxidant.[14]

The 3D structures of the above zeolites are invariably constructed via topotactic dehyoxylation between the layers in 2D lamellar precursors. The interlayer pore entrance, originally wide and open, then tends to be narrowed as a result of the condensation of hydroxyl groups and the removal of SDA molecules intercalated into the layers. More attractive applications are expected if new crystalline structures could be constructed by postsynthesis with expanded pore systems but still composed of the same framework units as the lamellar zeolites. Two useful techniques, that is, the phase delamination[15] and the interlayer pillaring with amorphous silica,[16] have then been developed to make full use of their potentially open porosity, together with the frameworks of zeolitic nature. Both delamination and pillaring are based on the swelling of the lamellar precursor with surfactant in advance, a procedure commonly used for the layered silicates. To cause structural swelling, the zeolitic lamellar precursors with more stable and stronger interlayer cross-linkages generally require much more severe conditions of the basic media. This then inevitably leads to a partial dissolution of the silicalite framework and also to a structural degradation.[17,18] Recently, it was reported that the swelling with surfactant and then the expansion of the interlayer spaces could be realized effectively at room temperature. This weak treatment at low temperature is considered to be advantageous to the preservation of the intralayer structure of the MCM-22 precursor.[18] Nevertheless, the swollen MCM-22 thus prepared is only useful for interlayer pillaring with silica, but is not suitable for delamination. Other new methods, which are capable of opening the porosity and constructing new crystalline structures but without destroying the basic building units, are urgently expected to widen the range of applications of these zeolites having lamellar precursors.

We report here a versatile method of converting 2D lamellar precursors into novel 3D crystalline metallosilicates according to a strategy of inserting a monomeric Si source into the interlayer spaces through one-step dialkoxysilylation followed by removal of the organic moieties. Such a simple soft-chemical methodology for expanding the pore structure avoids stepwise modifications such as interlayer expanding by ion-exchange with cationic surfactant, silylation, alcoholysis, and subsequent condensation, which are usually required for the nonzeolitic layered silicates.[19] The resulting materials with expanded pore windows, high crystallinity, and outstanding hydrothermal stability are proven to be active solid acid and redox catalysts for processing bulky molecules.

2. Experimental Section

2.1. Syntheses of Lamellar Precursors of Various Zeolites. Ti- or B-containing MWW lamellar precursor was hydrothermally synthesized using hexamethyleneimine (HMI) as an SDA from the gels with the molar compositions of 1.0 SiO_2: (0−0.033) TiO_2: 0.67 B_2O_3: 1.4 HMI: 19 H_2O following previously reported procedures.[14a] Using the same method described for the MWW-type ferrisilicate,[20] the MWW lamellar precursors containing Al, Ga, or Fe were synthesized from the gels of 1.0 SiO_2: 0.033 M_2O_3: 0.9 HMI: 0.15 Na_2O: 40 H_2O, where M represents Al, Ga, or Fe. The crystallization was carried out in Teflon-lined steel autoclaves under rotation (100 rpm) at 413 K for 7−10 days. The FER lamellar precursor, so-called PREFER, was hydrothermally synthesized using 4-amino-2,2,6,6-tetramethylpiperidine as an SDA following previously reported method.[5] The gel with the compositions of 1.0 SiO_2: 1.0 SDA: 1.5 NH_4F: 1.0 HF: 15 H_2O was crystallized in autoclave at 443 K for 7 days. The precursor of CDO topology, generally denoted PLS-1, was synthesized using tetramethylammonium hydroxide (TMAOH) as an SDA according to the literature method.[7] The gel with a composition of 1.0 SiO_2: 0.2 TMAOH: 18K_2O: 9 H_2O: 3.4 Dioxane was crystallized in autoclave under rotation at 423 K for 10 days. A pure silicalite precursor with the MCM-47 structure was synthesized using tetramethylene bis(*N*-methylpyrrolidinium) dibromide as an SDA, which was synthesized through the reaction of 1-methylpyrrolidine with 1,4-dibromobutane.[8] The product of lamellar precursor was crystallized from the gel with a composition of 1 SiO_2: 0.12 TMAOH: 0.30 NaOH: 40 H_2O at 443 K for 6 days.

All crystalline products were collected by filteration, washed repeatedly with deionized water, and then dried at 473 K overnight to obtain the lamellar precursors. A portion of precursor was calcined in air at 823 K for 10 h to burn off the occluded organic species to obtain corresponding zeolites with 3D structures.

2.2. Alkoxysilylation of Lamellar Precursors. The zeolite precursors were alkoxysilylated with $Me_2Si(OEt)_2$ under low pH conditions. Typically, 1 g of precursor was mixed with 50 g of aqueous solution of 2M HNO_3 and a desirable amount of $Me_2Si(OEt)_2$ (TCI). The mixture was then refluxed at 373 K for 20 h to induce the silylation. The solid-to-liquid weight ratio was always fixed at 1:50, while the amount of alkoxysilane was varied in the range of 0−0.3 g per gram of lamellar precursor. The silylated sample was filtered and washed with deionized water repeatedly and dried at 393 K for 10 h. The samples were further calcined in air at 823 K for 10 h to remove any organic species. The resulting interlayer expanded zeolites are denoted IEZ-ABC, where ABC represents the three letter code of the zeolite structure.

(13) Cheng, J. C.; Degnan, T. F.; Beck, J. S.; Huang, Y. Y.; Kalyanaraman, M.; Kowalski, J. A.; Loehr, C. A.; Mazzone, D. N. *Stud. Surf. Sci. Catal.* **1998**, *121*, 53–58.
(14) (a) Wu, P.; Tatsumi, T.; Komatsu, T.; Yashima, T. *J. Phys. Chem. B* **2001**, *105*, 2897–2905. (b) Wu, P.; Tatsumi, T.; Komatsu, T.; Yashima, T. *J. Catal.* **2001**, *202*, 245–255. (c) Song, F.; Liu, Y.; Wu, H.; He, M.; Wu, P.; Tatsumi, T. *J. Catal.* **2006**, *237*, 359–367. (d) Wang, L.; Liu, Y.; Xie, W.; Zhang, H.; Wu, H.; Jiang, Y.; He, M.; Wu, P. *J. Catal.* **2007**, *246*, 205–214.
(15) Roth, Q. J.; Kresge, C. T.; Vartuli, J. C.; Leonowicz, M. E.; Fung, A. S.; McCullen, S. B. *Stud. Surf. Sci. Catal.* **1995**, *94*, 301–308.
(16) Corma, A.; Fornés, V.; Pergher, S. B.; Maesen, Th; L. M.; Buglass, G. *Nature* **1998**, *396*, 353–440.
(17) Wu, P.; Nuntasri, D.; Ruan, J.; Liu, Y.; He, M.; Fan, W.; Terasaki, O.; Tatsumi, T. *J. Phys. Chem. B* **2004**, *108*, 19126–19131.
(18) Maheswari, S.; Jordan, E.; Kumar, S.; Bates, F. S.; Penn, R. L.; Shantz, D. F.; Tsapatsis, M. *J. Am. Chem. Soc.* **2008**, *130*, 1507–1516.
(19) (a) Mochizuki, D.; Shimojima, A.; Imagawa, T.; Kuroda, K. *J. Am. Chem. Soc.* **2005**, *127*, 7183–7191. (b) Mochizuki, D.; Kuroda, K. *New J. Chem.* **2006**, *30*, 277–285.
(20) Wu, P.; Ling, H.; Komatsu, T.; Yashima, T. *Chem. Commun.* **1997**, 663–664.

2.3. Characterization and Analysis Methods. Powder X-ray diffraction (XRD) patterns were collected on a MAC Science MX-Labo diffractiometer (Cu Kα radiation). The morphology was monitored by scanning electron microscopy (SEM) on a Hitachi S-5200 or S-4800 microscope. High resolution transmission electron microscopy (HRTEM) measurements were carried out with a 300 kV TEM (JEOL-3010, Cs = 0.6 mm, resolution 1.7Å). The ^{13}C and ^{29}Si MAS NMR spectra were recorded on a JEOL JNM ECA-400 multinuclear solid-state magnetic resonance spectrometer. IR spectra were collected on a Perkin-Elmer 1600 FTIR spectrometer at room temperature. The IR spectra in the hydroxyl stretching vibration region were measured after evacuating the self-supported wafers (30 mg of Ø 2 cm) at 557 K for 3 h, whereas the spectra in the framework vibration region were recorded using conventional KBr technique without evacuation. Elemental analyses of CHN were carried out on a Perkins-Elmer 2400 series II CHNS/O analyzer, while the amount of metals was quantified using inductive couple plasma mass spectroscopy on a Shimadzu ICPS-8000E-ICP instrument. UV−visible spectra were recorded on a JASCO V-550 spectrometer with a mode of diffusion reflectance using $BaSO_4$ as a reference.

2.4. Catalytic Reactions. The liquid-phase catalytic reactions were carried out in a 50 mL reactor equipped with a condenser and a magnetic stirrer. The epoxidation of cyclohexene with H_2O_2 was carried out using 0.05 g of catalyst, 10 mmol of substrate, 10 mmol of H_2O_2 (30 wt%),10 mL of MeCN at 333 K for 2 h. The Beckmann rearrangement of cyclohexanone oxime was carried out using 0.1 g of catalyst, 0.1 g of oxime, 20 g of PhCN solvent at 403 K for 2 h. The Baeyer−Villiger oxidation of cyclohexanone with H_2O_2 was carried out using 0.1 g of catalyst, 5 mmol of cyclohexanone, 2.5 mmol of H_2O_2 (30 wt%), and 4 mL of MeCN at 358 K for 3 h. The reaction products were analyzed on a Shimadzu GC-14B gas chromatograph equipped with an OV-1 capillary column and an FID detector. The amount of unconverted H_2O_2 was determined by the standard titration method with 0.1 M $Ce(SO_4)_2$ solution.

3. Results and Discussion

3.1. Interlayer Alkoxylation of Various Zeolite Lamellar Precursors. Various zeolitic lamellar precursors have been silylated with organic silanes in acidic media into highly ordered crystalline materials. Diethoxydimethylsilane (DEDMS) with two ethoxy groups was intentionally chosen to connect two up-and-down layers, possibly via the reaction with surface silanol groups; meanwhile, the two methyl groups would avoid intermolecular condensation. In the case of triethoxymethylsilane and tetraethoxysilane (TEOS), a serious condensation of silanes occurred, which may lead to the deposition of amorphous silica on the zeolite crystals. However, when dichlorodimethylsilane was employed as a silylating agent, very similar results to DEDMS were obtained. Figure 1 reports the XRD patterns of the lamellar precursors before and after direct calcinations, as well as after the silylation with DEDMS and further calcination. The precursors used were the titanosilicate for MWW structure and pure silicalites for the other zeolite structures. The XRD patterns of the precursors exhibited characteristic diffractions due to layered structures at lower angles (Figure 1a), which are in agreement with those reported in the literature.[4,5,7,8] The precursors were converted to corresponding 3D crystalline structures with so-called MWW, FER, CDO, and MCM-47 topologies, following a direct calcination in air, during which a

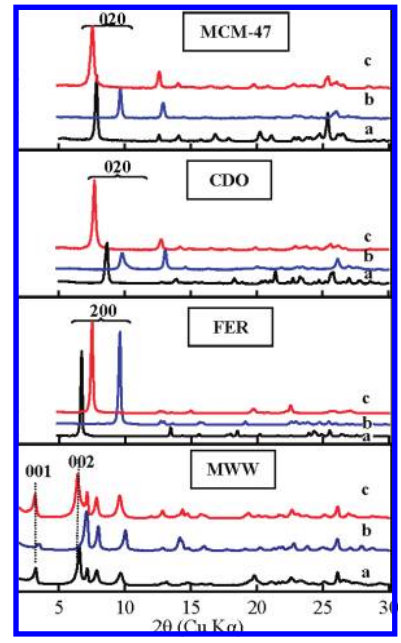

Figure 1. XRD patterns of various lamellar precursors (a), 3D zeolites formed by direct calcination of precursors (b), and interlayer expanded crystalline zeolites prepared by alkoxysilylation of precursors and further calcination (c). The structure code indicates the type of layer sheets.

common feature was observed in which the layer-related diffractions shifted to a higher 2θ region (Figure 1b). The structural changes essentially involved the burning off of the occluded organic SDA species, the condensation of the interlayer silanol groups, and the formation of cross-linkage between the layers. The direct calcination resulted in ordered 3D crystalline zeolite structures but a decrease in layer spacing, for example, from 26.93 to 25.09 Å for MWW. Thus, the calcined samples had a narrower pore entrance between the layers than that of the original lamellar precursors.

Nevertheless, when the precursors were silylated with DEDMS [$(EtO)_2SiMe_2$], crystalline and stable materials were obtained even after removing all organic species by calcination in air. In contrast to normal 3D zeolites obtained by direct calcination of the precursors, the silylated samples showed different but well-resolved XRD patterns in which the layer-related diffractions appeared in lower angles (Figure 1c). This indicates that an expansion of pore structure occurred at least between the layers. The structures changed mainly along the direction of layer stacking. These materials are nominated **i**nterlayer **e**xpanded **z**eolites (**IEZ**). The layer-related diffraction observed for both the precursor and the directly calcined sample was absent at the same 2θ position in the XRD pattern of silylated one (particularly obvious for FER, CDO, and MCM-47). This suggests that a homogeneous interlayer silylation occurred throughout the crystals and the IEZ sample was of phase purity rather than a composite structure of conventional 3D zeolite and interlayer-expanded material. Moreover, when the adjacent layers of the precursors were condensed upon direct calcination, the 3D structures formed had a relatively lower crystallinity (Figure 1b), probably due to a great strain of Si−O−Si bonds.[7,8] The phenomenon was paricularly observed for CDO and MCM-47. This was, however, not the case or less noticeable for corresponding IEZ samples, as they showed a higher crystallinity and well-defined diffractions. It seems that the stressing of the interlayer cross-linkages may be effectively relaxed by inserting

Table 1. Physicochemical Properties of Lamellar Precursors, Directly Calcined Samples and Interlayer Expanded Zeolites

		d-spacing /Å			surface area /m^2 g^{-1}	
original zeolites	*hkl*[a]	precursor	3D[b]	IEZ[c]	3D[b]	IEZ[c]
MWW	001	26.93	25.09	27.58	620	625
FER	200	13.07	9.36	11.75	403	410
CDO	020	10.20	9.12	11.47	300	438
MCM-47	020	11.25	9.16	11.51	312	410

[a] Representative layered structure-related plane. [b] Three-dimensional zeolites obtained by direct calcination of the precursors. [c] Interlayer expanded zeolites prepared by silylation of precursor with DEDMS and further calcination.

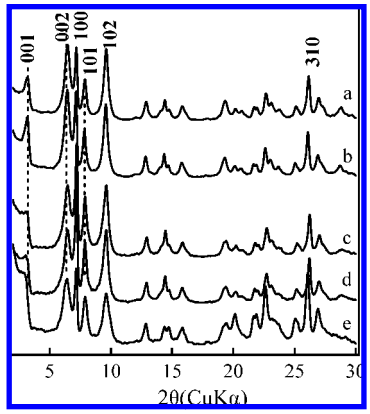

Figure 2. XRD patterns of various interlayer expanded metallosilicalites of IEZ-MWW. (a) borosilicate, (b) titanosilicate, (c) aluminosilicate, (d) gallosilicate, and (e) ferrisilicate. The samples were prepared by the silylation of corresponding MWW precursors with $Me_2Si(OEt)_2$ and then calcined.

the silicon species between the layers. This then contributed to a slight increase in specific surface area as shown next.

Table 1 summarizes the physicochemical properties of lamellar precursor, directly calcined samples, as well as silylated and subsequently calcined samples. The interlayer spacings were expanded by silylation by 2.3−2.5 Å in the IEZ samples. Considering the fact that the zeolites had relatively rigid structures inside the layers, the spacing expansion is presumed to mainly contribute to an enlargement of the pore windows between the layers. The N_2 adsorption at 77 K indicated that the IEZ samples had comparable or slightly higher specific surface areas in comparison to corresponding 3D zeolites obtained by directly calcining the precursors. This was in agreement with the above XRD patterns to verify that the IEZ samples were highly crystalline materials.

The synthesis strategy was also applicable to a variety of metallosilicalite precursors. Figure 2 shows the XRD patterns of the samples prepared by silylating the MWW precursors containing Ti, B, Al, Ga, or Fe after further calcination. After calcinations, all of the samples still showed clearly in the low angle region the resolved 001 and 002 diffractions due to an expanded layer structure, and also showed well-defined diffractions in the high angle region. In contrast, their precursors generally gave relatively broad diffractions in the high angle region (not shown) as reported previously.[14a,18] Different from interrupted interlayer connection in the precursors, these materials are thus considered to have a 3D crystalline structure rather than a 2D lamellar structure. Various metallosilicates having interlayer expanded pores were then prepared readily by inserting the silicon atoms between the layers.

The interlayer silylation did not change the coordination states of the framework metal ions. The IEZ-MWW titanosilicate

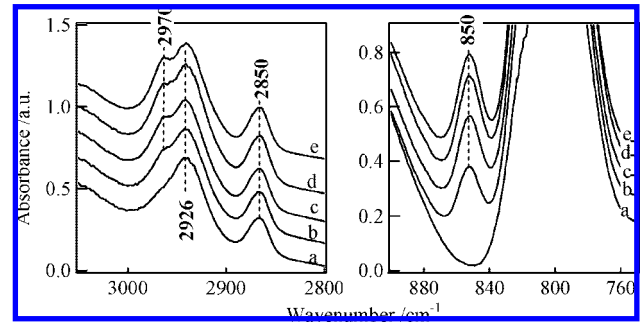

Figure 3. IR spectra of Ti-containing MWW lamellar precursor, after silylated with (a) 0 g, (b) 0.05 g, (c) 0.10 g, (d) 0.15 g, and (e) 0.30 g $Me_2Si(OEt)_2$ per gram of the precursor in 2 M HNO_3 without calcination.

showed a similar band at 220 nm to the conventional Ti-MWW in the UV−visible spectra, which is attributed to the charge transfer from oxygen atoms to Ti^{4+}, characteristic of tetrahedrally coordinated Ti in the framework.[21,22] However, the IR spectra in the region of hydroxyl stretching vibration showed the bands at 3620, 3630, and 3638 cm^{-1} for IEZ-MWW aluminosilicate, gallosilicate, and ferrisilicate, respectively (Supporting Information Figure S1). These bands are assigned to the structural Si(OH)M (M = Al, Ga, or Fe) groups,[20,23] indicating the presence of metal ions still in the framework. These silylated materials with opener pores may serve as potential solid acid with tunable Brønsted acidity for catalyzing the substrates with large molecular dimensions. Nevertheless, a demetalation took place to certain degree during the silylation, which is reasonably due to the treatment performed in an acidic media, in most cases 2M HNO_3. For example, the Si/Al ratio of 15 in the precursor of MCM-22 aluminosilicate changed to 35 in Al-IEZ-MWW after the silylation.

3.2. Investigation into Interlayer Alkoxysilylation with IR and Solid-State NMR. Concerning the degree of silylation, we have investigated the effect of silylation conditions such as treatment temperature, acid concentration, and particularly silane amount for all kinds of zeolite precursors mentioned in this work. Generally, a successful interlayer silylation preferred a refluxing treatment in 2M HNO_3. To reach a maximum silylation, the silylation was carried out under these conditions by varying the amount of DEDMS. IR spectroscopy was employed to monitor the silylation processes of lamellar precursors. Figure 3 shows the IR spectra of MWW precursor and silylated but uncalcined samples using a different amount of DEDMS. The precursor showed the bands at 2926 and 2850 cm^{-1} (Figure 3a), which are due to the stretching vibration of CH_2 groups originated from hexamethyleneimine (HMI), the SDA used for the crystallization of the precursor. The HMI molecules are reported to occupy both the interlayer space and the intralayer 10-MR channels.[24] The HMI molecules confined in the intralayer sinusoidal channels were hardly extracted by the acid treatment in silylation. Thus, the 2926 and 2850 cm^{-1}-bands were still observed after the silylation but decreased slightly in intensity. The silylation, however, developed new

(21) Vayssilov, G. N. *Catal. Rev. Sci. Eng.* **1997**, *39*, 209–216.
(22) Bellussi, G.; Rigguto, M. S. *Stud. Surf. Sci. Catal.* **2001**, *137*, 911–932.
(23) Corma, A.; Corell, C.; Pérez-Pariente, J. *Zeolites* **1995**, *15*, 2–8.
(24) Lawton, S. L.; Fung, A. S.; Kennedy, G. J.; Alemany, L. B.; Chang, C. D.; Hatzikos, G. H.; Lissy, D. N.; Rubin, M. K.; Timken, H.-K. C.; Steuernagel, S.; Woessner, D. E. *J. Phys. Chem.* **1996**, *100*, 3788–3798.

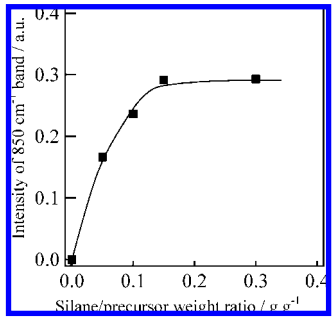

Figure 4. Dependence of the intensity of 850 cm^{-1}-band on the amount of $Me_2Si(OEt)_2$ used in the slilylation of MWW precursor.

bands at 2970 and 850 cm^{-1}, which are assigned as CH_3 asymmetric, stretching the rocking of CH_3 groups attached to Si.[25,26] This confirmed the incorporation of $(CH_3)_2Si$ moiety into the zeolite. The intensity of the 850 cm^{-1}-band increased with an increasing $Me_2Si(OEt)_2$ amount, but finally it leveled off at a silane to precursor weight ratio of 0.15 g g^{-1} (Figure 4), indicating a saturated incorporation of silane groups.

CHN elemental analyses indicated that the MWW precursor contained 10.23 wt% carbon and 2.03 wt% nitrogen species, corresponding to a C/N atomic ratio of 5.8. The value was very similar to the C/N ratio of HMI (6). The silylated sample prepared using 0.15 g silane relative to 1.0 g precursor contained 8.95 wt% carbon and 1.46 wt% nitrogen, showing a C/N atomic ratio of 7.2. The decrease in the total amount of organic species should be due to the removal of a part of the HMI, especially those located in interlayer spaces by acid extraction, while the increase in C/N ratio was gained by the incorporation of $(CH_3)_2Si$ groups. On the basis of a reduced amount of nitrogen, we could calculate the amount of carbon related to the HMI molecules removed by acid washing, and then the amount of carbon incorporated through the silylation. The maximum amount of $(CH_3)_2Si$ groups was 2.5 molecules per unit cell for MWW structure. According to the structure of MWW topology,[4] there are 2 pillaring sites per unit cell in the MWW precursor. It is thus deduced that the amount of $(CH_3)_2Si$ groups incorporated is enough to realize a complete and homogeneous interlayer silylation and then construct the cross-linkages between the layers. The extra $(CH_3)_2Si$ groups, corresponding to 0.5 molecules per unit cell, may be incorporated through reaction with the terminal silanols on the crystal surface or the internal silanols on the defect sites.

The treatment conditions optimized in the silylation of MWW precursor were also applicable to other precursors. Similarly, the silylation with DEDMS of the precursors of FER, CDO, and MCM-47 developed the silane group-related band at 850 cm^{-1} which was absent in the IR spectra of precursors (Figure 5).This confirmed the incorporation of $(CH_3)_2Si$ groups between the layers of these precursors.

The incorporation of $(CH_3)_2Si$ groups by the silylation of lamellar precursors has been further investigated by ^{13}C MAS NMR and ^{29}Si MAS NMR techniques. Figure 6A, trace a, reveals a typical ^{13}C MAS NMR spectrum of MWW precursor which showed three resonances at 57.0, 48.5, and 26.5 ppm. The former two resonances are attributed to the C_1 in HMI, while the latter one is attributed to the C_2 and C_3 in HMI.[24]

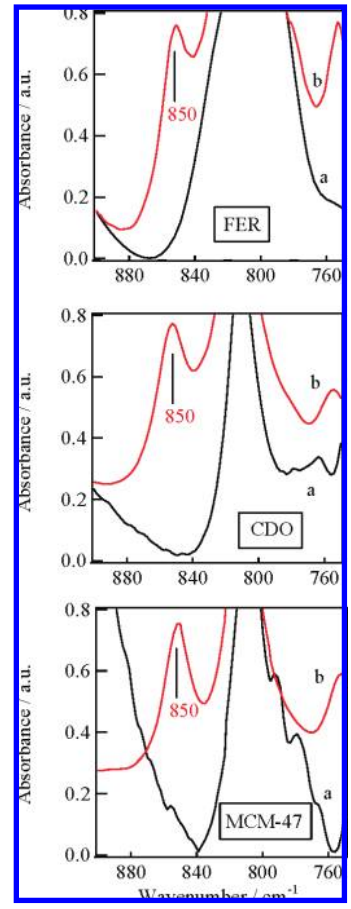

Figure 5. IR spectra of (a) lamellar precursors and (b) after silylated with $Me_2Si(OEt)_2$ in 2M HNO_3without calcination.

The presence of two resonances for C_1 of HMI is presumably associated with the residence of HMI in two distinct void spaces, that is, interlayer channels and intralayer channels. What is more attractive is that the silylation developed a new resonance at −2.0 ppm in^{13}C MAS NMR spectrum (Figure 6A, trace b), which is due to the configuration of $(CH_3)_2Si$ groups.[25]

In the case of the precursor of FER, multiple resonances were observed in the region of 20−60 ppm (Figure 6B, trace a). They are very similar to those reported previously and are attributed to the carbon atoms having different positions in the molecule of 4-amino-2,2,6,6-tetramethylpiperidine, the SDA used for the synthesis PREFER.[5] After the silylation, these resonances disappeared almost, while the resonance due to $(CH_3)_2Si$ appeared at −2.0 ppm (Figure 6B, trace b). Since the intralayer channels of PREFER, having only 8-MR pore windows, are not open enough to accommodate bulky molecules, the SDA with a relatively large molecular size is considered to be predominantly occluded inside the void spaces between the FER layers. Thus, in comparison to above HMI in the MWW precursor, the SDA molecules in PREFER were more easily removed by the acid refluxing during silylation. However, the precursor of CDO, so-called PLS-1, showed a single resonance at 56.9 ppm assigned to the SDA of tetramethylammonium (Figure 6C, trace a). This small cation wherever located was extracted readily and completely during the silylation and resulted in a spectrum in which the signal at 56.9 ppm was almost absent (Figure 6B, trace b). Meanwhile, the resonance due to $(CH_3)_2Si$ was again visible at −2.0 ppm, confirming the interlayer silylation. Interestingly, the silylated PREFER also

(25) Joo, J.; Hyeon, T.; Hyeon-Lee, J. *Chem. Commun.* **2000**, 1487–1488.
(26) Yamamoto, K.; Nohara, Y.; Domon, Y.; Takahashi, Y.; Sakata, Y.; Plévert, J.; Tatsumi, T. *Chem. Mater.* **2005**, *17*, 3913–3920.

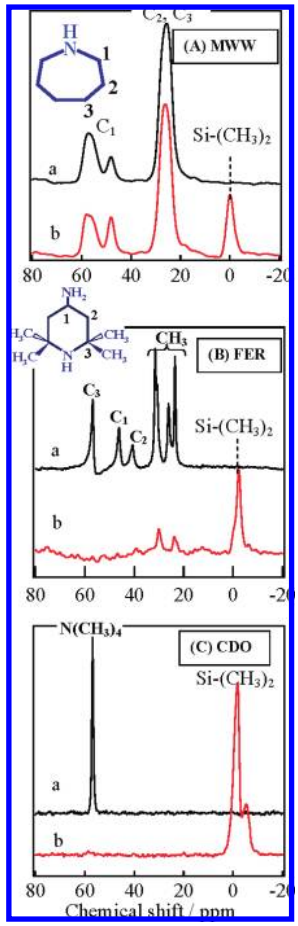

Figure 6. ^{13}C MAS NMR spectra of (a) lamellar precursors and (b) after silylated with $Me_2Si(OEt)_2$ in 2M HNO_3without calcination.

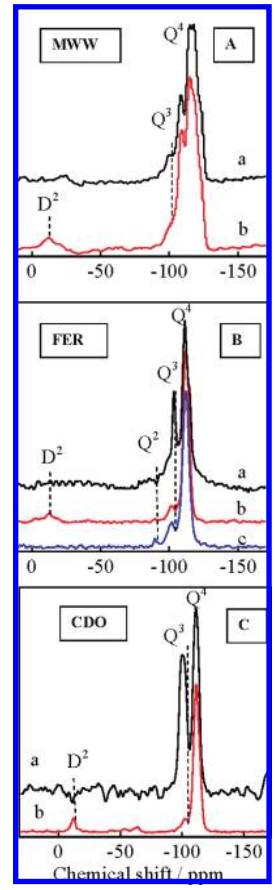

Figure 7. ^{29}Si MAS NMR spectra. (a) lamellar precursor, and (b) after silylated with $Me_2Si(OEt)_2$ in 2M HNO_3without calcination, and (c) silylated sample after calcination.

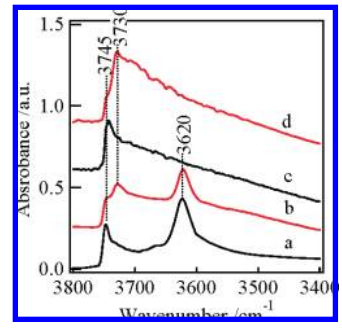

Figure 8. IR spectra in hydroxyl stretching region of (a) Al-MCM-22 (Si/Al = 15), (b) Al-IEZ-MWW, (c) FER silicalite, and (d) IEZ-FER after evacuation at 773 K for 2 h.

showed a signal at −5.4 ppm in the ^{13}C MAS NMR spectrum. This resonance could be due to (i) the $(CH_3)_2Si$ groups located in different places other than interlayer spaces, and /or (ii) the CH_3Si groups formed by losing a methyl group in $(CH_3)_2Si$ as a result of decomposition under refluxing conditions. When we carried out the silylation of PLS-1 at a higher temperature, such as 443 K in a sealed autoclave, the resonance at −5.4 ppm became more intense, while the resonance at −2.0 ppm became weaker (Supporting Information Figure S2). This result allows us to tentatively assign the resonance at −5.4 ppm to the silane groups losing a CH_3 group, that is, CH_3Si unit.

Figure 7 shows the ^{29}Si MAS NMR spectra of various lamlellar precursors before and after alkoxysilylation with DEDMS. For all precursors, the main resonances at −110 and −120 ppm were from silicon atoms coordinated with four silicon atoms (Q^4). A distinguished resonance at −103 ppm was also particularly observed for the precursors of FER and CDO. This resonance is attributable to the silicon-bearing OH groups, $(OH)Si(SiO)_3$ (Q^3),[5] indicating the precursors contained abundant silanol groups on the layer surface. After the silylation, the Q^3 resonance decreased greatly in intensity, while the samples exhibited a new resonance at −15 ppm at the expense of Q^3 groups (Figure 7A−C, trace b). This signal is attributed to the silicon atom from $Si(CH_3)_2(OSi)_2$ groups (D^2).[27] The results clearly indicate that the silylation occurred through the reaction of silane groups with the silanols on the layer surface to form pillaring silicon species between the layers.

Using silylated PREFER as an example, we have investigated the effect of calcination on the structural change. After burning off the organic species by calcination in air, the D^2 resonance disappeared instead of forming a more intensive signal at −92 ppm (Figure 7B, trace c).This resonance could be assigned to $Si(OH)_2(OSi)_2$ groups (Q^2)[28] or 3MR Q^3 units possibly formed through the polymerization of $Me_2Si(OEt)_2$ to cyclic silane species.[27] It is very difficult for us to directly differentiate two kinds of signals having very similar chemical shifts. To clarify

(27) Engelhardt, G.; Michel, D. *High-Resolution Solid-State NMR of Silicates and Zeolites*; John Wiley & Sons Ltd.:New York, 1987.

(28) Woolery, G. L.; Alemany, L. B.; Dessau, R. M.; Chester, A. W. *Zeolites* **1986**, *6*, 14–16.

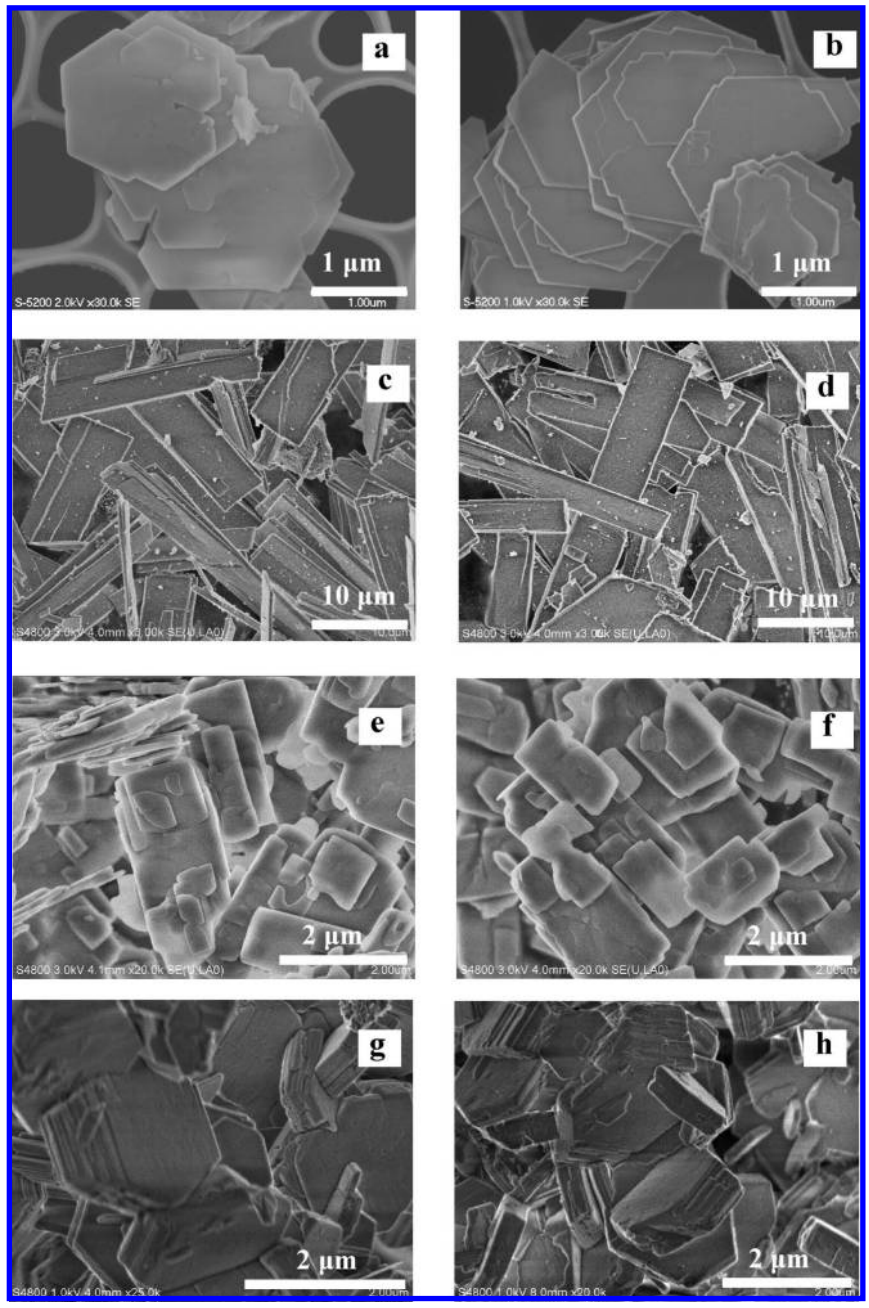

Figure 9. SEM images of (a) 3D MWW, (b) IEZ-MWW, (c) FER, (d) IEZ-FER, (e) CDO, (f) IEZ-CDO, (g) MCM-47, and (h) IEZ-MCM-47.

this issue, we have compared the silylation between the FER lamellar precursor (uncalcined) and the 3D FER silicalite (directly calcined sample of precursor) under the same conditions. If the polymerization and cyclization of $Me_2Si(OEt)_2$ actually occurred in the treatment, the silylated 3D FER silicalite should gave similar signal at −92 ppm. Nevertheless, in contrast to the silylation of precursor which developed new signals at −12 ppm and −92 ppm after calcination, the silylation of the calcined silicalite already with the 3D FER structure led to the same ^{29}SiMAS NMR spectra as the parent (Supporting Information Figure S3). No additional resonances due to D^2, Q^2, and/or 3MR Q^3 signals were developed at −12 and −92 ppm. This would rule out the possibility of the formation of 3MR Q^3 units and their contribution to the −92 ppm-resonance. In fact, the elemental analyses indicated that the amount of silane incorporated by silylation was 2.15 mmol g^{-1} for the lamellar precursor and 0.13 mmol g^{-1} for the 3D FER silicalite, respectively. The content of the latter was much lower. The IR spectra also revealed that the 850 cm^{-1} band was almost invisible for the silylated 3D FER (Supporting Information Figure S4). The precursor and 3D FER silicalite differed mainly in the interlayer silanol groups. Above results suggest not only that the silane molecules were hardly incorporated once the interlayer silanols were condensed by calcination to construct the 3D FER structure, but also that the silane was not polymerized to deposit on the crystal surface or inside the pores. Thus, we could exclude the formation of cyclic or other types of siloxanes in silylation and then assign the −92 ppm-signal to Q^2 group rather than 3MR Q^3 group. The Q^2 group−groups resulted from the incorporated $Si(CH_3)_2(OSi)_2$ by losing two methyl groups in calcination. These results clearly verified that the alkoxysilyl groups actually condensed with the silanols on

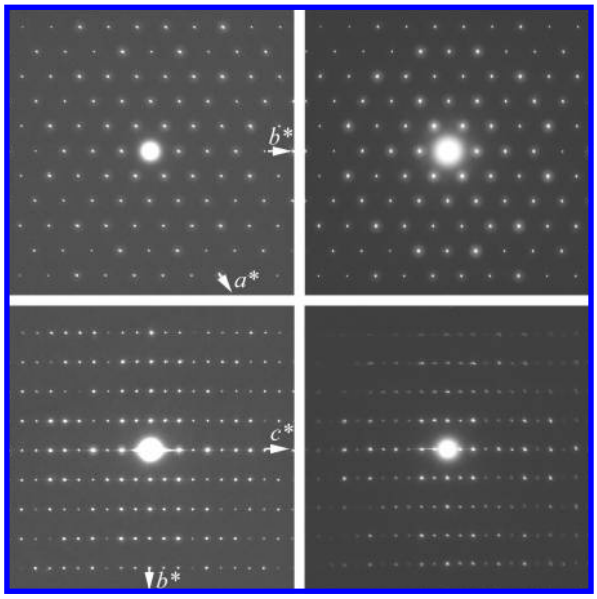

Figure 10. Selected area electron diffraction patterns of 3D MWW (left column) and IEZ-MWW (right column) along [001] and [100] directions.

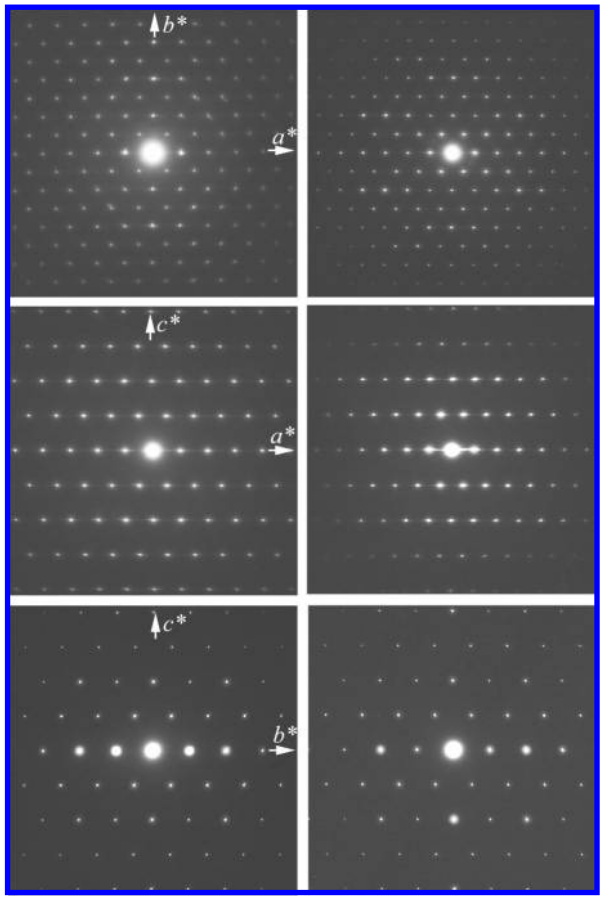

Figure 11. Selected area electron diffraction patterns of 3D FER (left column) and IEZ-FER (right column) along [001], [010], and [100] directions.

the layer surface to create new Si−O−Si linkages, which contributed to the interlayer expansion.

IR spectroscopy also gave us consistent evidence for the formation of Q^2 groups in the silylated and further calcined samples. Figure 8 shows the IR spectra in the hydroxyl stretching vibration region of pure silica 3D FER and IEZ-FER as well as 3D MWW MCM-22 aluminosilicate and corresponding Al-IEZ-MWW. The 3D FER showed a main band at 3745 cm^{-1} due to terminal silanols. In addition to the 3745 cm^{-1}-band, the 3D MCM-22 showed an another band at 3620 cm^{-1} due to the framework Al(OH)Si groups.[23] The interlayer silylation of MWW and FER lamellar precursors with $Me_2Si(OEt)_2$ developed, in both cases, a new band at 3730 cm^{-1}, which was nearly invisible for corresponding 3D MWW and FER counterparts, but made the bands at 3745 and 3620 cm^{-1} almost intact. The 3730 cm^{-1}-band was ascribed to a kind of internal silanols,[29] probably corresponding to a kind of hydrogen-bonded geminal $=Si(OH)_2$ groups. These results were in agreement with above Q^2 signal observed in above ^{29}Si MAS NMR spectra, giving a strong evidence for the incorporation of $Si(CH_3)_2(OSi)_2$ groups introduced by silylation first and then formation of silicon species bearing silanols in following calcination.

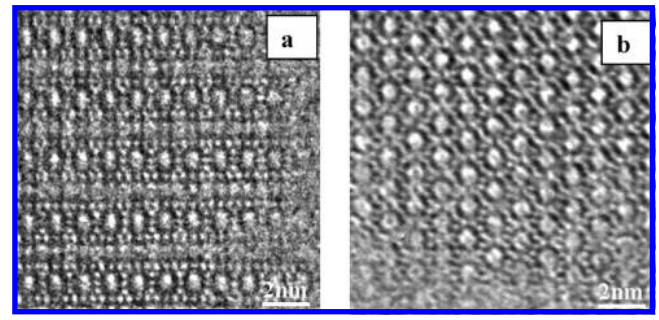

Figure 12. HRTEM images of calcined IEZ-MWW (a) and IEZ-FER (b) taken along the direction of layer stacking.

3.3. Electron Microscopy Investigation. Figure 9 shows the SEM images of various 3D zeolites and corresponding IEZ materials. The crystals of these materials were all thin flakes, which, however, were different in shape and size in terms of their fundamental zeolite structures. A direct calcination of the precursor, and silylation and subsequent calcination did not result in any significant changes to the crystal morphology. Although the XRD patterns clearly evidenced a structural expansion along the direction of layer stacking after the silylation (Figure 1), the SEM images gave no information concerning the changes in crystal thickness. Thus, the formation of new crystalline structure by silylation took place not through destroying and reconstructing the macro crystals but at an atomic or molecular level.

The structural changes as a result of silylation have been investigated by HRTEM measurement on two IEZ structures. Figure 10 and Figure 11 show the selected area diffraction patterns of 3D MWW and IEZ-MWW, 3D FER and IEZ-FER along two or three main directions, respectively. They revealed that IEZ materials had very similar pore arrays and sizes within the layers to the 3D structures obtained by direct calcination. However, as evidenced by the *d*-spacing measured by HRTEM (Supporting Information Table S1), the well-ordered pores were expanded along the direction perpendicular to the layers in the IEZ samples, that is, along the [001] direction for IEZ-MWW and [200] for IEZ-FER. The values of pore expansion were in agreement with the data obtained by XRD shown in Table 1.

(29) Fan, W.; Wu, P.; Namba, S.; Tatsumi, T. *J. Catal.* **2006**, *243*, 183–191.

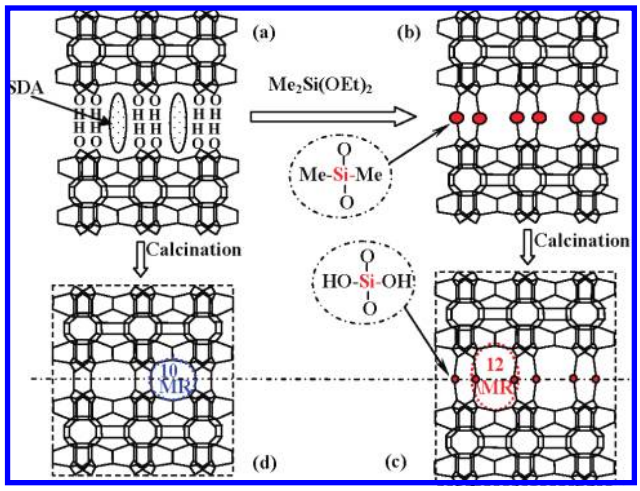

Figure 13. Sequence of postsynthesizing interlayer expanded zeolites through dialkoxysilylation of lamellar precursor (using MWW precursor as a representative). (a) MWW lamellar precursor, (b) the interlayer structure expanded via the reaction of silane with silanols on the layer surface, (c) formation of a novel ordered 3D crystalline structure with enlarged pore window in comparison to normal 3D MWW structure, and (d) common 3D MWW structure obtained by a direct interlayer dehydroxylation.

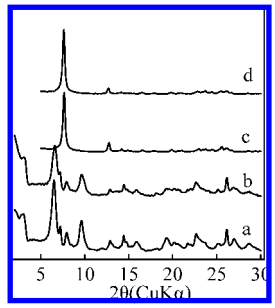

Figure 14. XRD patterns of IEZ-MWW (aluminosilicate) before (a) and after (b) refluxed in boiling water for 6 days IEZ-FER (pure silicalite); (c) and after (d) refluxed in boiling water for 15 days .

The TEM images have been examined carefully and randomly in the regions of crystals, which evidenced that the pores were enlarged along the layer stacking direction uniformly. The XRD patterns noted earlier evidenced already that the IEZ materials were almost free of the phases owing to the precursors and the 3D structures obtained by direct calcination. This should be ascribed to a maximum degree of interlayer silylation was realized after optimizing the silylation conditions, particularly the amount of alkoxysilane (Figures 2 and 4).

The number of tetrahedral atoms of the aperture of interlayer pores increased by two, e.g. forming 12-MR pores in both IEZ-MWW and IEZ-FER (vis-a-vis 10-MR pores of 3D MWW and FER) as showed by the enlarged HRTEM images along the layer stacking direction (Figure 12). In the case of IEZ-MWW, XRD, and HRTEM verified that it was very similar to previously reported Ti-YNU-1, which has been obtained only by chance when a postsynthesized Ti-containing MWW precursor with an extremely low Ti content (generally Si/Ti >70) was acid-treated.[30a] The present method, however, is proved to be more general, neither depending on the precursor types nor the metal content.

3.4. Possible Mechanism for Interlayer Silylation and Pore Expansion. The above results allow us to propose a possible mechanism for constructing new zeolite structures through interlayer silylation of lamellar precursors. Figure 13 depicts the sequence using MWW precursor as an example. In silylation, the DEDMS molecules react with silanol groups attached to the layer surface to realize incorporation of monomeric silane groups and formation of Si−O−Si linkages between the layers (Figure 13, parts a and b). The subsequent calcination burns off the methyl groups coordinated to the Si, as well as SDA species occluded in the pores, leading to a new pore structure pillared mainly by $Si(OH)_2$ groups (Figure 13c). The silylation thus makes the number of interlayer pore window increase by two in comparison to directly calcined precursor (Figure 13d). We cannot deny the possibility of forming partially the Si−O−Si connection between the neighboring silane groups in case of the zeolite structures making them close to each other. To understand this complicated issue, a final structural resolution is needed for particular case.

3.5. Hydrothermal Stability of IEZ Materials. The thermal stability of IEZs should not be taken as an important issue, as their structures survived the calcination at 823 K in air. Nevertheless, although the Si species incorporated effectively pillar the layers and cross-link the layers to enlarge the interlayer pores, both ^{29}SiMAS NMR and IR investigation showed that those Si species are not tetrahedrally coordinated to four Si atoms, but contain a part of OH groups, mostly existing in $Si(OH)_2$ configuration. This would increase the hydrophilicity of resulting materials and bring about hydrothermal stability problem. We thus have investigated the hydrothermal stability of IEZ by refluxing the samples in water. As shown by XRD patterns (Figure 14), there were no obvious decrease in intensity and changes in diffraction position when IEZ-MWW and IEZ-FER were boiled at 373 K in water for 1−2 weeks. The diffractions due to expanded layer structures were still observed in the low angle region, indicating that the structures were totally preserved. The high hydrothermal stability of IEZ is presumably contributed by the pillaring Si species firmly connected to the layers.

3.6. Catalytic Properties of IEZ Materials. The IEZ materials, having larger pores than the 3D structure obtained by direct calcination, are expected to show higher catalytic activities for bulky molecules. Using MWW metallosilicates as representatives, the catalytic properties of IEZ thus have been investigated in processing bulky molecules as both redox and solid acid catalysts. In comparison to their counterparts with conventional 3D MWW topology, Ti-containing IEZ-MWW catalysts showed much higher conversion and specific activity (turnover number per Ti active site) in cyclohexene oxidation with H_2O_2 (Supporting Information Table S2). This reaction is reported to require large-pore zeolites as effective catalysts.[14b] Additionally, Al and Ga-containing IEZ-MWW catalysts were superior to their 3D MWW counterparts in Beckmann rearrangement of cyclohexanone oxime and Baeyer−Villiger oxidation of cyclohexanone with H_2O_2, respectively (Supporting Information Table S2). Both reactions involving cyclic substrates and products are considered to require open reaction spaces.[31−33] The activity improvement should be contributed by the silylation which created opener pores between the layers. The IEZ catalysts,

(30) (a) Fan, W.; Wu, P.; Namba, S.; Tatsumi, T. *Angew. Chem., Int. Ed.* **2004**, *43*, 236–240. (b) Ruan, J.; Wu, P.; Slater, B.; Terasaki, O. *Angew. Chem., Int. Ed.* **2005**, *44*, 6719–6723.
(31) Camblor, M. A.; Corma, A.; García, Semmer-Herlédan, V.; Valencia, S. *J. Catal.* **1998**, *177*, 267–272.
(32) Ngamcharussrivichai, C.; Wu, P.; Tatsumi, T. *J. Catal.* **2004**, *227*, 448–458.
(33) Corma, A.; Nemeth, L. T.; Renz, M.; Valencia, S. *Nature* **2001**, *412*, 423–425.

possessing much open reaction spaces, were thus easily accessible to the substrates with large molecular dimensions and also advantageous to product desorption.

4. Conclusions

A methodology has been demonstrated for postsynthesizing new crystalline zeolites with enlarged pores through alkoxysilylating various zeolitic lamellar precursors. The interlayer structures of MWW, FER, CDO, and MCM-47 topologies are expanded successfully by the silylation of corresponding precursors. The structural transformation is independent of the metallosilicate types and the metal contents. The resulting materials evolve to ordered crystalline structures having opener pore windows and a high thermal/hydrothermal stability. The construction of structures is realized as a result of inserting monomeric silane source forming Si−O−Si linkages between the layers. These materials, composed of the building units identical to directly calcined precursors but exhibit larger porosity, not only serve as effective heterogeneous catalysts for large molecules, but also are expected to provide promising selective adsorbents for adsorption and separation.

Acknowledgment. National Natural Science Foundation of China (20673038), NCET-04-0423 Science and Technology Commission of Shanghai Municipality (STCSM) (06SR0710 and 06dj14006), 973 Program (2006CB202508), and Shanghai Leading Academic Discipline Project (B409) are thanked for funding (PW). Supports from Swedish Research Council, VR, and Japanese Science and Technology Agency, JST, are acknowledged (OT and TT).

Supporting Information Available: IR, ^{13}C and ^{29}Si MAS NMR spectra, *d*-spacing values obtained by HRTEM and the results of catalytic reactions. This material is available free of charge via the Internet at http://pubs.acs.org.

JA0758739